

# Numerical Study of the Flow Around the S818-NR Aerodynamic Profile Based on Modern Turbulence Models

*Sardorbek Muzaffarov*<sup>1,3\*</sup>, *Jura Jumayev*<sup>2</sup>, *Shukhratjon Turayev*<sup>2</sup>, *Maftuna Avazxonova*<sup>2</sup>

<sup>1</sup>Institute of Mechanics and Seismic Stability of Structures named after M.T. Urazbaev, Tashkent, Uzbekistan

<sup>2</sup>Bukhara State University, Bukhara, Uzbekistan

<sup>3</sup>Oriental University, Tashkent, Uzbekistan

**Abstract.** This study examines the subsonic airflow around a S818-NR air foil at angles of attack from 0° to 20° through numerical simulation. The calculations were done in COMSOL Multiphysics using the finite element method. The Shear Stress Transport (SST) model was used to accurately capture the complicated nature of turbulence. We got numerical results for important aerodynamic parameters like lift coefficient, pressure distribution, and velocity components. A comparative analysis of various Reynolds numbers was performed to assess their impact on the flow structure. The simulation results were very similar to the experimental data, which showed that the chosen turbulence model and numerical method were reliable. The data collected help us better understand how turbulent flow works around aerodynamic profiles, and they can be used to design and improve wind turbines.

## 1 Introduction

Turbulent flow is a basic but very complicated fluid mechanics phenomenon that happens when particles move in an irregular and chaotic way. It comes from nonlinear interactions in the fluid, which makes predicting and mathematically modelling it one of the hardest problems in modern physics and engineering. Turbulence is very important in aerodynamics because it affects lift, drag, and the overall stability of airplanes, as well as the efficiency of wind turbine blades. In hydrodynamics, it controls how water moves in rivers, channels, and pipelines. This has a direct effect on how hydraulic systems are built and how well they work. Many aspects of turbulence are still not fully understood, even though computational and experimental studies have made a lot of progress. So, studying and simulating turbulent flows is still a big part of current research. This work is helping to create better aerodynamic designs and renewable energy technologies. Numerous studies have focused on the examination of airflow around aerodynamic profiles. Specifically, the research in [3] centres on improving the performance of wind turbines by using numerical models to study how the blades move through the air. The results show that changing the

---

\* Corresponding author: [sardorbekmuzaffarov50@gmail.com](mailto:sardorbekmuzaffarov50@gmail.com)

shape and angle of attack of an airfoil is the most important thing you can do to make it more energy efficient. Simulations done with changing flow conditions and velocity fields made it possible to see streamlines and parameter distributions. This helped improve the design of wind turbine blades. The aerodynamic properties of helicopter air foils NACA 0012, NACA 23012, VR12, and HH02 were studied numerically in [5] at different angles of attack and Mach numbers. RANS-based simulations in ANSYS Fluent took into account the effects of transition, stall, and flow compressibility. The results we got, such as pressure coefficient distributions and integral aerodynamic parameters, matched what we found in experiments. A comparative analysis revealed aerodynamic trends beneficial for optimizing blade geometry and enhancing CFD modelling of rotorcraft profiles. The aerodynamic properties of S-series air foils (S809, S811, S814, S818) were examined in [7] utilizing ANSYS Fluent. The study looked at Reynolds numbers and angles of attack between  $0^\circ$  and  $20^\circ$ . The results showed that the S811 and S818 profiles are more aerodynamically efficient because they create more lift while creating less drag. These profiles also have weaker vortex wakes and less turbulence, which makes them good for use in wind turbine blades. Using the SST Mentor and RNG  $k-\epsilon$  turbulence models, unsteady RANS simulations were done on the NREL S809 airfoil in [9]. We looked at fully turbulent flow conditions at attack angles from  $0^\circ$  to  $20^\circ$ . We got the lift and drag forces by adding up the surface pressure and shear stress. The comparison showed that the SST Mentor model is better at predicting turbulent flow around the air foil. Zhang et al. [10] conducted a numerical investigation of the S809 airfoil utilizing a two-dimensional finite-difference solver for both steady and unsteady, compressible viscous flows, grounded in the Reynolds-averaged Navier–Stokes (RANS) equations. We looked at four different two-equation turbulence models, some of which were linear and some of which were not. Simulations were conducted at a designated Reynolds number and angles of attack varying from  $0^\circ$  to  $70^\circ$ . The results demonstrated acceptable accuracy up to the stall region; however, significant discrepancies from experimental data were noted beyond the stall. Du and Selig [12], along with Hu et al. [13], examined the three-dimensional rotational effects on blades originating from the S809 airfoil, whereas Chaviaropoulos and Hansen [14] evaluated the NACA63-4XX and NACA63-2XX blade profiles. Their results showed that blade rotation slows down flow separation, and Hu et al. [13] stressed how important Coriolis and centrifugal forces are in causing three-dimensional stall delay. Even though a lot of research has already been done in this area, studying the aerodynamic properties of rotor and wind turbine blades is still an important and difficult scientific problem. The primary objective of this study is to examine the airflow behaviour around helicopter and wind turbine blade profiles by solving the Reynolds-averaged Navier–Stokes (RANS) equations and to ascertain both local and integral aerodynamic parameters across a broad spectrum of angles of attack. From an engineering point of view, air foils that are 10–18% thicker than average are very important because they are in the middle of rotor and wind turbine blades. These parts are very important for determining how well and efficiently the blade works while it is in use. The U.S. National Renewable Energy Laboratory (NREL) made the S818-NR airfoil for small and medium-sized wind turbines. It demonstrates high aerodynamic efficiency and operational stability at low and moderate wind speeds, making it suitable for variable wind environments and distributed energy systems.

You can use the work's results to make the shapes of wind turbine blades, helicopter rotor blades, and other aerodynamic shapes. Simultaneously, by assessing the aerodynamic efficiency of the profile at low, medium, and high Reynolds numbers and various angles of attack, a scientific foundation was established for enhancing energy efficiency, minimizing flow separation, and improving aerodynamic stability.

## 2 About the S818-NR profile

The S818-NR air foil has a maximum relative thickness of about 18%, which gives it high structural strength and aerodynamic efficiency because it has a good lift-to-drag ratio. It can handle high angles of attack without losing flow, and the design takes into account the laminar–turbulent transition, which makes flow more stable and energy conversion more efficient. But there are still some important things that haven't been studied enough, like maximum lift, flow separation zones, and how the air behaves at different Reynolds numbers and angles of attack. The goal of this work is to use the COMSOL Multiphysics software to look into these factors numerically. Simulations of turbulent flow around the S818-NR profile at angles of attack ranging from  $0^\circ$  to  $20^\circ$  will enhance comprehension of its aerodynamic efficiency and the potential for optimizing wind turbine design. Aerodynamic analysis is necessary for making wind turbines work better and designing them. Because it is so efficient and stable, the S818-NR air foil is one of the most popular profiles. Computational Fluid Dynamics (CFD) makes it possible to simulate airflow in great detail under different operating conditions. This helps find important aerodynamic parameters like lift, drag, and flow separation. This research utilizes the Shear Stress Transport (SST) turbulence model to resolve the Navier–Stokes equations and examine turbulent flow around the S818-NR profile at various angles of attack. We compare the numerical results we get with experimental data to see how accurate and reliable the model is. This helps us improve the design of wind turbine blades.

### 3 Physical and Mathematical Formulation of the Problem

The turbulent flow around the S818-NR air foil is examined under nearly incompressible flow conditions. The chord length determines the Reynolds number. Figure 2 shows the computational mesh that was used in the numerical simulation.

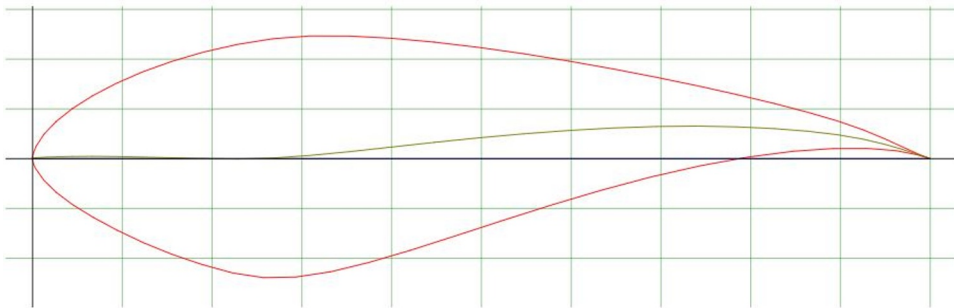


**Fig. 1.** 2D S818-NR Profile.

Using the commercial software COMSOL Multiphysics, this study simulated the flow around a two-dimensional aerodynamic profile. The analysis utilized the unsteady Reynolds-averaged Navier–Stokes (RANS) equations, predicated on a steady, incompressible, and two-dimensional flow. These equations provide the fundamental mathematical framework for incompressible fluid dynamics, describing the spatial and temporal variations of velocity and pressure in the flow field. The SST  $k$ - $\omega$  turbulence model was chosen to give a more accurate picture of how the flow behaves because it is not completely turbulent.

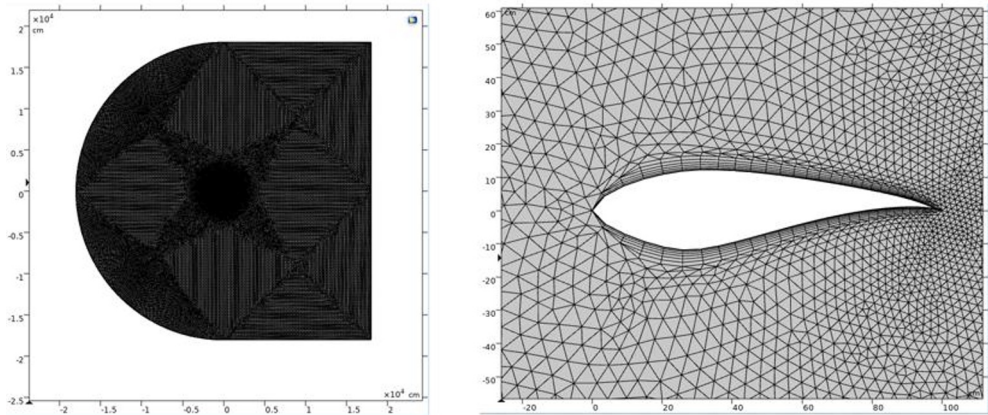


**Fig. 2.** Computational Mesh.

This model, which combines the best parts of the  $k-\epsilon$  and  $k-\omega$  formulations, makes it easier to predict boundary-layer separation and effects near walls. We used a fully coupled solution approach to make sure that the pressure and velocity fields were properly linked. We also used a second-order discretization scheme for both the pressure and momentum equations.

The main equations used in the study are as follows:

The continuity equation was solved using a steady-state approach:

$$\frac{\partial(\rho U_j)}{\partial x_j} = 0 \quad (1)$$

Time-averaged momentum equation:

$$\frac{\partial \rho U_j U_i}{\partial x_j} = -\frac{\partial P}{\partial x_j} + \frac{\partial}{\partial x_j} \left( \mu \frac{\partial U_i}{\partial x_j} \right) + \frac{\partial}{\partial x_j} (-\rho u_i' u_j') \quad (2)$$

## 4 Turbulence Model

Menter (1994) came up with the SST (Shear Stress Transport)  $k-\omega$  model, which combines the best parts of the  $k-\epsilon$  and  $k-\omega$  models. It is one of the most popular models for modelling the flow around air foils because of the following benefits. The  $k-\omega$  model is very accurate near the wall, and the SST model gives the best answer because the velocity gradients in the boundary layer and the turbulence levels that change quickly. The point where the flow separates is very important for aerodynamics, especially for profiles that aren't symmetrical. The SST model does the best job of modelling separation, reclosure zones, and flow when the system is in stall mode. The SST model employs a shear stress-limiting transport mechanism, facilitating stable computations at elevated Reynolds numbers. The SST model is well-known for being very accurate. It has been compared to many experimental results on NASA [10], S-series, DU, and other air foils. It costs less to run than LES or DES models, but it is more accurate than RANS models. The SST Menter model is a mix of the and models. The method uses the model close to the wall, but then it switches to the model farther away from the wall (i.e., closer to the outer edge of the boundary layer) using a special function.

Equation is changed into the form (see [4]). This approach makes it possible to exploit the advantages of both models:

The model doesn't need wall corrections and gives a better picture of flows with a bad pressure gradient. But the answer depends on the values of the turbulent variables in the outside flow, especially on [8]. The model is less sensitive to these variables, but requires modification near the wall.

Menter's SST model has been shown to give much better results when simulating flows with a strong adverse pressure gradient than the original and models (Kral [1]). Kral [1] says that the model works better because it uses Menter's turbulent viscosity limiter. Catalano and Amato point out that Menter's SST  $k-\omega$  formulation is one of the best turbulence models for predicting the sharp flow separation seen in experiments. The results are similar to those of nonlinear models, but the SST model is less rigid and works better with computers. This turbulence model has been shown to work well for simulating isolated wing flows, and it has also been used successfully for the aerodynamic analysis of wind turbine systems.

The model is built on these two transport equations:

Turbulent kinetic energy:

$$\frac{\partial(\rho k)}{\partial t} + \frac{\partial(\rho U_i k)}{\partial x_i} = \frac{\partial}{\partial x_j} \left[ (\mu + \sigma_k \mu_t) \frac{\partial k}{\partial x_j} \right] + P_k - \beta^* \rho \omega \quad (3)$$

Specific dissipation  $\omega$  :

$$\frac{\partial(\rho \omega)}{\partial t} + \frac{\partial(\rho U_j \omega)}{\partial x_j} = \frac{\partial}{\partial x_j} \left[ (\mu + \sigma_\omega \mu_t) \frac{\partial \omega}{\partial x_j} \right] + \alpha \frac{\omega}{k} P_k - \beta \rho \omega^2 + 2(1 - F_1) \rho \sigma_{\omega 2} \frac{1}{\omega} \frac{\partial k}{\partial x_j} \frac{\partial \omega}{\partial x_j} \quad (4)$$

The following formula is used to determine the turbulent viscosity in the SST  $k - \omega$  model:

$$\mu_t = \frac{\rho k}{\omega} \frac{1}{\max\left(1, \frac{\alpha^* \omega}{5F_2}\right)} \quad (5)$$

The coefficient  $P_k$  indicates the rate at which turbulent energy  $k$  is generated in the flow as a result of velocity shear or flow deformation:

$$P_k = \mu_t \left( \frac{\partial U_i}{\partial x_j} + \frac{\partial U_j}{\partial x_i} \right) \frac{\partial U_i}{\partial x_j} \quad (6)$$

The SST  $k - \omega$  model employs two key switching functions -  $F_1$  and  $F_2$  that determine which turbulence model is applied in different flow regions.

$F_1$  - is active in the near-wall regions and ensures the use of the  $k - \omega$  model close to the wall. This function is particularly important for the accurate simulation of laminar-to-turbulent transition and shear layers, where the  $k - \omega$  model provides more precise results:

$$F_1 = \tanh \left( \left[ \min \left( \max \left( \frac{\sqrt{k}}{\beta^* \omega y}, \frac{500v}{y^2 \omega} \right), \frac{4\rho \sigma_{\omega 2} k}{CD_{k\omega} y^2} \right) \right] \right) \quad (7)$$

$F_2$  begins to dominate in regions away from the wall, facilitating a smooth transition to the  $k - \varepsilon$  model. This is important in free-stream regions, where the  $k - \varepsilon$  model more accurately represents turbulence:

$$F_2 = \tanh \left( \left[ \max \left( \frac{\sqrt{k}}{\beta^* \omega y}, \frac{500v}{y^2 \omega} \right) \right] \right) \quad (8)$$

In (7) and (8)  $\rho$  – denotes the density;  $U$  – is the velocity vector;  $\mu$  – represents the molecular (dynamic) viscosity;  $\mu_t$  – turbulent viscosity;  $P_k$  – source term of turbulent kinetic energy,  $y$  – distance to the nearest wall (m),  $\alpha$ ,  $\beta$ ,  $\beta^*$ ,  $\sigma_k$ ,  $\sigma_\omega$ ,  $\sigma_{\omega 2}$  – model constants;  $CD_{k-\omega}$  – modified diffusion term:

$$CD_{k-\omega} = \max\left(\frac{2\rho\sigma_{\omega 2}}{\omega} \nabla k \cdot \nabla \omega, 10^{-10}\right) \quad (9)$$

where  $\nabla k \cdot \nabla \omega$  is the scalar product of the gradients of  $k$  and  $\omega$ . The closure of the system requires the use of the equation of state for a perfect gas.

$$p = \rho RT \quad (10)$$

where  $R$  is the specific gas constant for air.  $T=293,15 K$  – air temperature. For the considered cases, the Reynolds number was.

$$Re = \frac{\rho u_0 l}{\mu} = \frac{1.2043 \cdot 20 \cdot 1}{1.81397 \cdot 10^{-5}} = 1.327805 \cdot 10^6 \quad (11)$$

which corresponds to a developed turbulent flow regime over a solid surface. Thus, a value of  $\mu = 1.81397 \cdot 10^{-5} \frac{kg}{m \cdot s}$  was adopted in the calculations. Accordingly, the turbulence model was selected.

To model how turbulence affects the flow around the S818-NR air foil, the Reynolds-averaged Navier–Stokes (RANS) equations are used. We used the finite element method in COMSOL Multiphysics to run numerical simulations that let us look closely at the flow structure and how it behaves aerodynamically. This study looks at how well the SST turbulence model can predict turbulent flow around the S818-NR air foil. To make sure the model is correct, the numerical results are compared to experimental data from the NASA Turbulence Modelling Resource (TMR) database [11].

The boundary conditions on the semicircle and on the  $y = \pm 20 m$  boundaries (at the  $G_1$  boundary, Fig. 2) are specified depending on the angle of attack.

$$U(x_{G1}, y_{G1}) = U_0 \cos \alpha, \quad V(x_{G1}, y_{G1}) = U_0 \sin \alpha, \quad (12)$$

where  $U_0$  – is the velocity magnitude of the incoming free-stream flow;  $\alpha$  is the angle between the flow direction and the OX coordinate axis.

At this boundary, the value of the excess pressure is equal to zero:

$$p(x_{G1}, y_{G1}) = 0 \text{ (Pa)} \quad (13)$$

Accordingly, for the boundary

$$G_2 = (0 \leq x \leq 1) \cap (y = f_1(x) \cup f_2(x))$$

$$f_1(x) = 0.01627 + 0.54375 \cdot x - 2.95464 \cdot x^2 + 6.52378 \cdot x^3 - 6.41245 \cdot x^4 + 2.28547 \cdot x^5$$

$$f_2(x) = -0.00636 - 0.29824 \cdot x + 1.35819 \cdot x^2 + 2.61152 \cdot x^3 - 2.24646 \cdot x^4 - 0.69 \cdot x^5$$

the conditions were specified.  $U(x_{G2}, y_{G2}) = V(x_{G2}, y_{G2}) = 0 m/s$

At the outlet of the computational domain  $y = \pm 2.0 \text{ m}$  ( $G_3$ ), a smooth matching condition was applied to determine the velocities.

$$\frac{\partial U(x_{G3}, y_{G3})}{\partial n} = 0, \quad \frac{\partial V(x_{G3}, y_{G3})}{\partial n} = 0 \quad (12)$$

## 5 About the COMSOL Multiphysics program and its capabilities

The COMSOL Multiphysics program uses numerical methods to solve different aerodynamic and hydrodynamic problems. It lets you model the flow around airfoils, find the pressure and velocity fields, and figure out aerodynamic coefficients. The program has been changed so that it can calculate both laminar and turbulent flows. This lets you find out how the flow behaves at different Reynolds numbers and angles of attack. Camsol SST uses new turbulence models like  $k-\omega$  that accurately model separation zones, stalling, and reclosing. At the same time, the program allows you to adjust the type, density and degree of clustering of the grid around the profile, which is important for fully reflecting the physical properties of the flow. Using Camsol, we can figure out the lift and drag coefficients, the pressure distribution, and how the flow structure changes over time. This lets us figure out how aerodynamic and stable the profile is. So, Camsol has a lot of potential for numerical modeling of the flow around the S818-NR profile at different Reynolds numbers and attack angles in this work. This makes it possible to get reliable and accurate results from both experimental and theoretical data.

## 6 Solution Method

For the standard SST turbulence model, the standard solvers of COMSOL Multiphysics were used.

The computations were carried out for  $50000 < \text{Re} < 1000000$  at various angles of attack within the range of  $0 \leq \varphi \leq 20^\circ$ .

As shown in Fig. 1, local mesh refinement was used in the calculations near the surface of the  $f1(x)$  and  $f2(x)$  profile.

The area around the air foil that was being calculated was broken up into a mesh with 50600 elements. The quality of the computational grid is very important for accurately modelling the flow around an aerodynamic profile. This is because the grid type, element density, and total number of cells all affect how well the physical characteristics of the flow are captured. So, the choice of grid was based on certain physical needs, available experimental data, and well-known international standards.

During the simulations, different mesh configurations with different densities and clustering strategies were tried out. It was found that the chosen mesh configuration most accurately reproduced the flow features by comparing how they affected important aerodynamic parameters like pressure distribution, lift and drag coefficients, and separation behaviour. So, this study's final computational results were all based on this best mesh arrangement.

A suitable relaxation coefficient was used to make sure that the solution converged steadily. We used a steady-state approach to solve the problem, starting with the potential flow solution as the first guess.

The finite volume method first finds velocity fields for a set time step. Then, to keep mass conservation, it uses the Poisson equation to find pressure corrections.

The program usually ran for two hours or more. The outputs included fields of longitudinal and transverse velocities, pressure fields, turbulent kinetic energy and its dissipation, and aerodynamic derivatives.

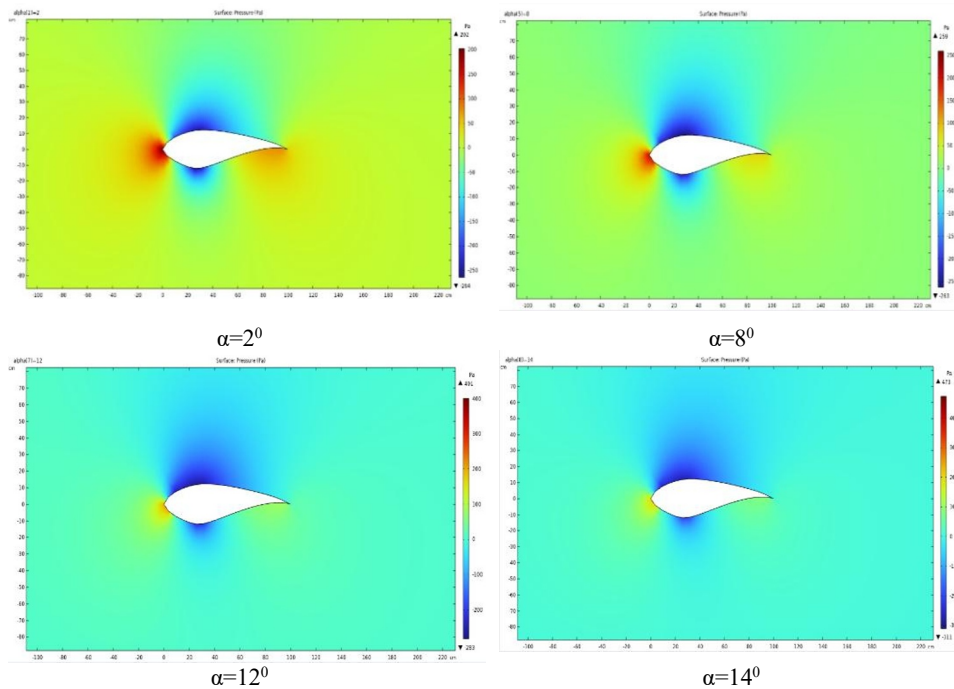
The following quantities were used as input data for the calculation: wind speed in m/s, angular speed in rad/s, air density in kg/m<sup>3</sup>, and pressure in (see Table. 1).

**Table 1.** Input data window with dimensions and initial values.

Parameters		
Name	Expression	Value
$U_{\text{inf}}$	$20[\text{m} \cdot \text{s}^{-1}]$	20 m/s
$\rho_{\text{inf}}$	$1.2043[\text{kg} \cdot \text{m}^{-3}]$	1.2043 kg/m <sup>3</sup>
$\mu_{\text{inf}}$	$1.81397\text{e-}5[\text{kg} \cdot \text{m}^{-1} \cdot \text{s}^{-1}]$	1.81397E-5 kg/(m*s)
L	20[m]	20 m
C	1[m]	1 m
$k_{\text{inf}}$	$0.1 \cdot \mu_{\text{inf}} \cdot U_{\text{inf}} / (\rho_{\text{inf}} \cdot L)$	1.5062E-6 m <sup>2</sup> /s <sup>2</sup>
$\omega_{\text{inf}}$	$10 \cdot U_{\text{inf}} / L$	10 1/s
Alpha	0	0
Re	$U_{\text{inf}} \cdot c \cdot \rho_{\text{inf}} / \mu_{\text{inf}}$	1.3278E6

## 7 Results and Discussion

It is important to make pressure field isolines at different angles of attack for aerodynamic analysis because it lets you see how the pressure is spread out around the airfoil and judge its properties. Using the pressure isolines we got (Fig. 3), we looked at how the pressure changed on the air foil at different angles of attack.



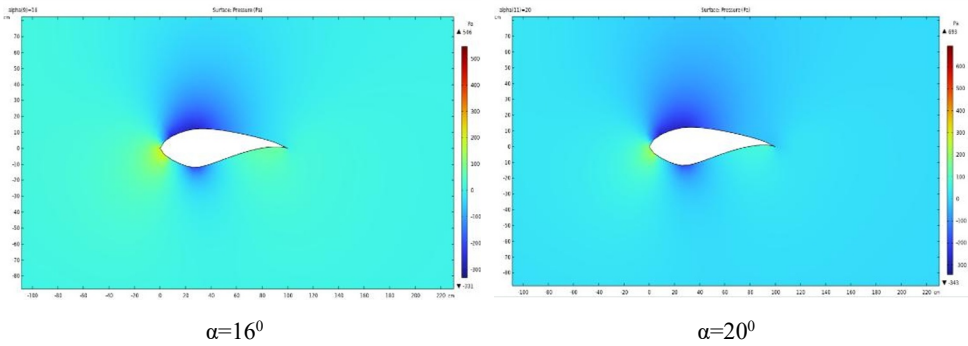


**Fig. 3.** Pressure field isolines at different angles of attack

At  $\alpha=2^\circ$ , the flow goes over the air foil more smoothly, creating a low-pressure area on the top surface (shown in blue) that helps lift the air foil. The flow near the air foil stays stable.

The low-pressure area becomes clearer when  $\alpha=8^\circ$ . There is a big drop in pressure on the upper surface near the leading edge, which means that the lift coefficient (CL) goes up.

The lift is almost at its highest point when  $\alpha=12^\circ$ . The pressure difference between the top and bottom surfaces becomes important, showing that the air foil is at its most aerodynamically efficient.

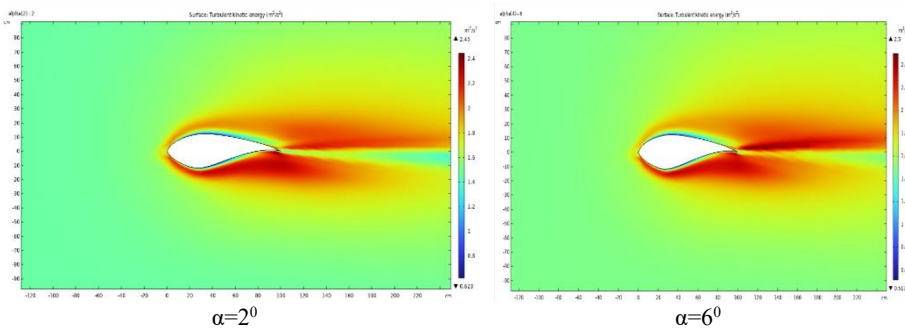
When  $\alpha=14^\circ$ , flow separation starts to happen on the upper surface. The lift is still high, but the area where the lift is separated starts to get bigger. This could make the lift less efficient.

At  $\alpha=16^\circ$ , the separation region becomes clear: reverse flow starts to form on the top surface, which makes lift go down.

When  $\alpha=20^\circ$ , most of the upper flow breaks away from the airfoil surface. In this case, the flow stalls, which means that the lift drops sharply and the drag coefficient (CD) goes up a lot. This makes the air foil's aerodynamic performance go down a lot.

The best angle of attack for this air foil is about  $\alpha=10^\circ\sim 12^\circ$ . When the angle is greater than  $14^\circ$ , the flow separation region gets bigger, which makes the lift go down and the aerodynamic efficiency go down. The analysis makes it easy to see how the lift and drag forces change and to find the flow stability boundary around the air foil.

It is important to look at the turbulent kinetic energy isolines (Fig. 4) around the airfoil at different angles of attack to see how the flow works and how well the airfoil works.



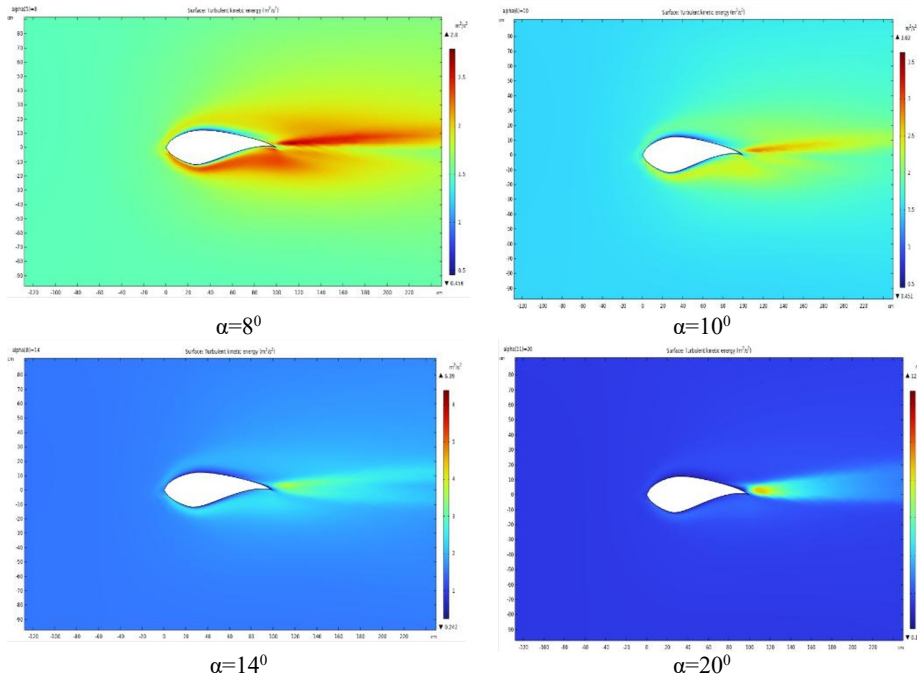


**Fig. 4.** Turbulent kinetic energy isolines of the flow at different angles of attack

Turbulent kinetic energy (TKE) is a key measure for figuring out how unstable a flow is, where separation zones are, and how they affect aerodynamic efficiency. Here is an analysis of how the TKE distribution changes at different angles of attack  $\alpha$ :

At  $\alpha=2^\circ$ , there isn't much turbulence, and only a little bit of turbulent energy can be seen near the flow exit. The flow is in a stable aerodynamic state, with almost no separation region. This means that it is almost laminar.

The turbulence region starts to grow at  $\alpha=6^\circ$ , especially along the top surface of the airfoil. There is more turbulent energy in the wake region behind the airfoil, which means that flow separation is starting to happen.

When  $\alpha=8^\circ$ , the turbulent energy on the top surface goes up a lot. The separation zone moves down, and the flow in the wake becomes less stable. This means that aerodynamic losses are going up.

The level of turbulence goes down at  $\alpha=10^\circ$ , which could mean that the flow stability is getting better. In this regime, the lift stays high, and the turbulent energy moves away from the airfoil. This state is about the best for aerodynamic efficiency.

At  $\alpha=14^\circ$ , it is easy to see that the flow is separating along the upper surface, and the turbulent area is moving toward the back. This shows that the flow is starting to stall and the aerodynamic efficiency is going down.

When  $\alpha=20^\circ$ , the turbulent kinetic energy close to the airfoil drops sharply, but the separation region gets wider and stays that way. This is what happens when the lift drops quickly and the drag goes up a lot, which is typical of full flow stall.

The analysis indicated that the ideal aerodynamic regime, determined by turbulent kinetic energy, is found within the interval of  $\alpha=6^\circ\sim 10^\circ$ . When  $\alpha$  is greater than  $14^\circ$ , the flow becomes unstable, the aerodynamic efficiency goes down, and the separation areas get bigger. This kind of assessment is an important part of controlling the flow, finding aerodynamic losses early, and cutting down on them.

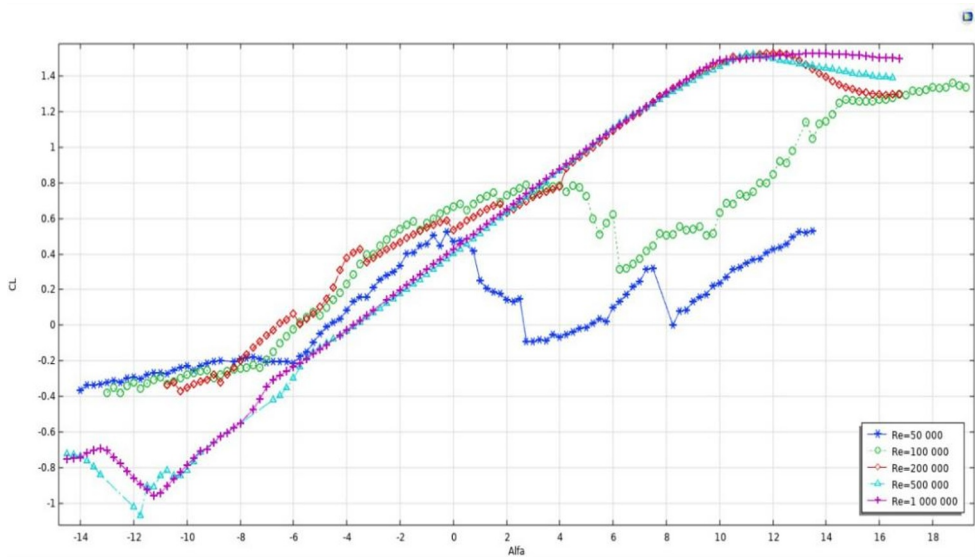


**Fig. 5.** Analysis of the lift coefficient  $C_L$  as a function of the angle of attack.

The following patterns can be observed from the graph.

For all values of  $Re$ , an increase in  $C_L$  is observed with the rising angle of attack up to approximately  $10^0$ – $12^0$ . At  $Re = 500000$  and  $Re = 1000000$ , this increase occurs smoothly and steadily, reaching a maximum value of  $C_L \approx 1.4$ . After reaching the maximum, flow separation occurs, causing  $C_L$  to drop sharply. At low  $Re$ , for example at  $Re = 50000$ , separation occurs early - around  $6^0$ . At  $Re = 100000$  and  $200000$ , the separation is less pronounced. At high  $Re$  ( $500000$  and  $1000000$ ), the decline of  $C_L$  is less abrupt, indicating a high aerodynamic stability of the airfoil.

At negative angles of attack ( $\alpha < 0$ ),  $C_L$  takes negative values, indicating the generation of downward lift. In this range, the behaviour of  $C_L$  also depends on the Reynolds number: at higher  $Re$  values, the airfoil better resists laminar flow separation. Thus, at high Reynolds numbers ( $Re \geq 500000$ ), the S818-NR airfoil demonstrates high aerodynamic efficiency, with significant  $C_L$  values, smooth flow separation, and stable lift growth. At the same time, at low  $Re$  ( $\leq 100000$ ), early laminar separation limits the growth of  $C_L$  and reduces the airfoil's efficiency.

## 8 Conclusion

The scientific novelty of this study is that the flow properties of an asymmetric aerodynamic profile at different Reynolds numbers were studied based on modern turbulent models. The pressure distribution around the profile, the change in lift and drag coefficients, as well as the formation of separation zones and their dependence on the Reynolds number were analysed in detail. At the same time, aerodynamic properties that were not sufficiently covered in previous experiments, such as the evolution of the flow structure in different regimes, the conditions for the onset of the stall process, and the sensitivity to high pressure gradients, were revealed. As a result, new scientific conclusions were developed regarding the aerodynamic efficiency of an asymmetric profile at low, medium, and high Reynolds numbers.

In the article, the standard SST  $k-\omega$  turbulence model from the COMSOL Multiphysics software package, which uses the finite element method, was used to simulate the flow

around the S818-NR aerodynamic profile. Velocity fields, pressure coefficients, and other parameters were analysed.

The SST  $k-\omega$  model does a good job of predicting both the lift and drag for the S818 airfoil. The experiment works best when the angle of attack is between  $12^\circ$  and  $14^\circ$ . The model can be used to do numerical aerodynamic analysis of this airfoil with moderate angles of attack.

Engineers and designers can learn a lot from using CFD methods to study how air flows around the S818-NR aerodynamic profile. You can use this information to make wind turbines and airplanes more efficient, improve the shape of the profile, and improve the aerodynamic efficiency. Using numerical modelling to learn about the profile's aerodynamic properties helps create new technologies that will help businesses use more renewable energy.

The profile has low aerodynamic drag, which helps save fuel and make planes go faster. It is made to reduce turbulence, which makes the plane more stable and easier to control.

The S818-NR aerodynamic profile is a very effective way to design wind turbine blades. Its geometric and aerodynamic properties provide high lift, low drag, and excellent aerodynamic performance, making it an ideal choice for modern wind turbines.

## References

1. L. D. Kral, "Recent experience with different turbulence models applied to the calculation of flow over aircraft components," *Progress in Aerospace Sciences*, **34**, 481–541 (1998).
2. D. Yu. Evseev and O. K. Ovchinnikova, "Numerical Simulation of the Flow around an Aerodynamic Profile and Wind Turbine Blade," *Aerospace Engineering and Technologies*, **1** (1), 117–130 (2023) (in Russ.).
3. F. R. Menter, "Two-equation eddy-viscosity turbulence models for engineering applications," *AIAA Journal*, **32** (8), 1598–1605 (1994).
4. A. L. Tarasov, "Numerical Study of the Flow Features of Helicopter Airfoils in the Operational Range of Angle of Attack and Mach Number Variations," *MAI Proceedings*, **131**, (2023). DOI: 10.34759/trd-2023-131-13. (in Russ.).
5. X. Li, K. Yang, L. Zhang, J. Bai and J. Xu, "Large thickness airfoils with high lift in the operating range of angle of attack," *Journal of Renewable and Sustainable Energy*, **6**, 033110 (2014).
6. M. J. Hamzah, L. Al-Sadawi, A. Khudhair and T. Biedermann, "Aerodynamic characteristics evaluation of S-series airfoils," *Engineering and Technology Journal*, **41**, (2023).
7. M. M. Hamdamov, R. A. Fayziyev and S. S. Muzaffarov, "Numerical simulation of wind turbines conducted using COMSOL software," *E3S Web of Conferences*, **541**, 01001 edited by D. Nazarov, A. Juraeva va S. Talu (Almaty, Kazakhstan, 2024).
8. O. Guerri, K. Bouhadef and A. Harhad, "Turbulent flow simulation of the NREL S809 airfoil," *Wind Engineering*, **30** (4), 287–302 (2006).
9. S. Zhang, X. Yuan and D. Ye, "Analysis of turbulent separated flows for the NREL airfoil using anisotropic two-equation models at higher angles of attack," *Wind Engineering*, **25**, 41–53 (2001).
10. Turbulence Modeling Resource, NASA Langley Research Center. URL: <http://turbmodels.larc.nasa.gov>

11. Z. Du and M. S. Selig, “The effect of rotation on the boundary layer of a wind turbine blade,” *Renewable Energy*, **20** (2), 167–181 (2000).
12. D. Hu, O. Hua and Z. Du, “A study on stall-delay for horizontal axis wind turbine,” *Renewable Energy*, **31**, 821–836 (2006).
13. P. K. Chaviaropoulos and M. O. L. Hansen, “Investigating three-dimensional and rotational effects on wind turbine blades by means of a quasi-3D Navier–Stokes solver,” *ASME Journal of Fluids Engineering*, **122**, 330–336 (2000).
14. P. Fuglsang and C. Bak, “Development of the Riso wind turbine airfoils,” *Wind Energy*, **7**, 145–162 (2004).